J|A|C|S ARTICLES

Published on Web 03/26/2009

Nitrogen-Rich Heterocycles as Reactivity Retardants in Shocked Insensitive Explosives

M. Riad Manaa,* Evan J. Reed, Laurence E. Fried, and Nir Goldman

Lawrence Livermore National Laboratory, Energetic Materials Center, P.O. Box 808, Livermore, California, 94551

Received October 17, 2008; E-mail: manaa1@llnl.gov

Abstract: We report the first quantum-based multiscale simulations to study the reactivity of shocked perfect crystals of the insensitive energetic material triaminotrinitrobenzene (TATB). Tracking chemical transformations of TATB experiencing overdriven shock speeds of 9 km/s for up to 0.43 ns and 10 km/s for up to 0.2 ns reveal high concentrations of nitrogen-rich heterocyclic clusters. Further reactivity of TATB toward the final decomposition products of fluid N_2 and solid carbon is inhibited due to the formation of these heterocycles. Our results thus suggest a new mechanism for carbon-rich explosive materials that precedes the slow diffusion-limited process of forming the bulk solid from carbon clusters and provide fundamental insight at the atomistic level into the long reaction zone of shocked TATB.

Many high explosives are organic molecular crystals that contain both oxidizing and reducing functional groups. These solids rapidly release their energy in supersonic detonation waves. The reaction times of high explosives inferred from hydrodynamic measurements can be as fast as a few nanoseconds or as long as many microseconds.[1] The molecular processes responsible for the reaction times (also referred to as a reaction zone length) are not understood. It has been observed, however, that explosives rich in carbon tend to have much longer reaction zones than those that do not. These explosives form graphitic or diamond-like carbon particles during detonation.[2−4] The slow process of forming the bulk solid from large carbon clusters is believed to play a central role in determining the size of the reaction zone of a given explosive.[2,5] The latter process is thought to be initiated by collecting carbon atoms from a relatively large volume and governed by diffusion-limited growth of these clusters. In this work, we identify an altogether new mechanism for the slow reactivity of carbon-rich explosives. We present quantum-based multiscale simulations of shocked 1,3,5-triamino-2,4,6-trinitrobenzene (TATB) which provide the first evidence for the formation of an extended region of nitrogen-rich heterocyclic clusters, the formation of which further impede reactivity toward final decomposition products of fluid N_2 and solid carbon.

TATB ($C_6H_6N_6O_6$) is one of the most insensitive explosives known, with an estimated reaction zone in the microsecond regime. TATB exhibits strong intramolecular and intermolecular hydrogen bonds in a graphite-like crystal structure (see Figure 1b), which maybe responsible for the extraordinary stability of TATB under thermal, impact, or shock initiation.[6] These strong interactions are manifested in molecular TATB by a hydrogen bond that is in the range of 1.7−1.8 Å between neighboring oxygen−hydrogen at the equilibrium structure, giving rise to relatively large torsional barriers for the amino and nitro groups (17 and ∼6 kcal/mol, respectively, at the MP2 level of theory).[7] Furthermore, having the same number of atoms among its atomic constituents, TATB can be described as markedly underoxidized, or alternatively, carbon rich. As a consequence, significant carbon formation in some form (graphite, clusters, or diamond) is one of the final products of TATB under detonation reactions.

We simulate crystal TATB's reactivity under steady overdriven shock compression using the multiscale shock technique.[8,9] In this molecular dynamics (MD) method, equations of motion for the atoms and volume of the computational cell are time evolved subject to stress and energy constraints satisfying a continuum description of the shock wave. Since the computational cell of the multiscale technique follows a lagrangian point through the shock wave, it enables a simulation of a system experiencing a shock wave with far fewer atoms than normally required by the direct method of inducing a shock wave in a very large computational cell. In tandem, the use of quantum-based methods to calculate interatomic forces allows reliable predictions of chemical reactions, while providing insights into the electronic structure and chemical transformations of the reacting system for a relatively long time-scale on the order of several hundreds of picoseconds.[10]

(1) Mader, C. L. *Numerical Modeling of Detonations*; University of California: Berkeley, CA, 1979.
(2) Shaw, M. S.; Johnson, J. D. *J. Appl. Phys.* **1987**, *62*, 2080.
(3) Nomura, Y.; Kawamura, K. *Carbon* **1984**, *22*, 189.
(4) Greiner, N. R.; Philips, D. S.; Johnson, J. D.; Volk, F. *Nature (London)* **1988**, *333*, 440.
(5) Viecelli, J. A.; Ree, F. H. *J. Appl. Phys.* **1999**, *86*, 237.
(6) Dobratz, B. M. *The Insensitive High Explosive Triaminotrinitrobenzene (TATB): Development and Characterization-1888 to 1994*; Los Alamos National Laboratory: Los Alamos, NM, 1995.
(7) Manaa, M. R.; Gee, R. H.; Fried, L. E. *J. Phys. Chem. A* **2002**, *106*, 6606.
(8) Reed, E. J.; Fried, L. E.; Joannopoulos, J. D. *Phys. Rev. Lett.* **2003**, *90*, 235503.
(9) Reed, E. J.; Fried, L. E.; Manaa, M. R.; Joannopoulos, J. D. In *Chemistry at Extreme Conditions*; Manaa, M. R., Ed.; Elsevier: New York, 2005; pp 297−326.
(10) Reed, E. J.; Manaa, M. R.; Fried, L. E.; Glaesemann, K. R.; Joannopoulos, J. D. *Nat. Phys.* **2008**, *4*, 72.
(11) Cady, H. H.; Larson, A. C. *Acta Crystallogr.* **1965**, *18*, 485.

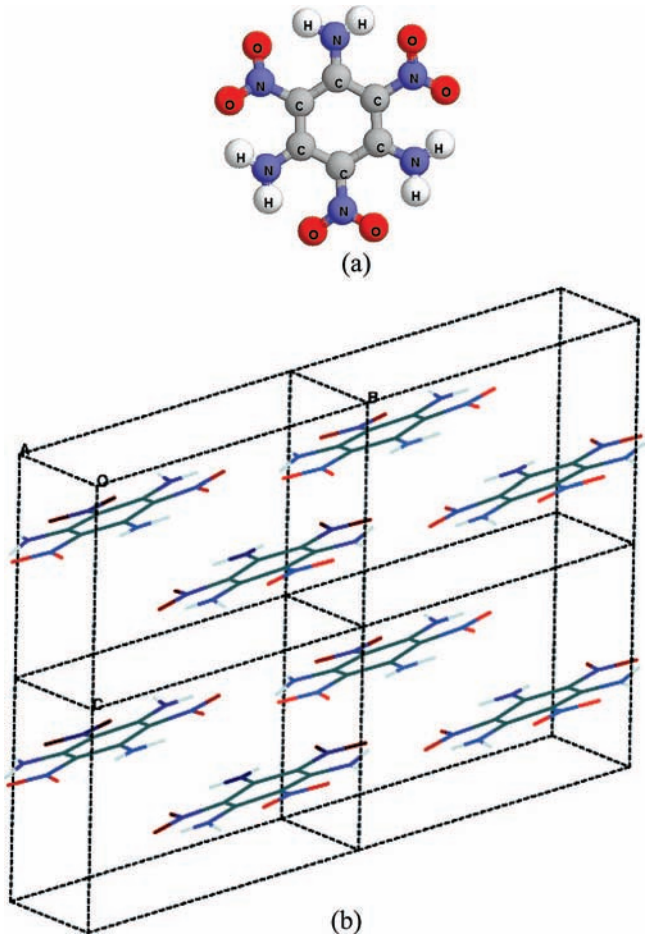

Figure 1. (a) Molecular TATB ($C_6H_6N_6O_6$). (b) Graphite-like sheets in a $1 \times 2 \times 2$ supercell of nonorthorhombic crystals of TATB solid phase. The X-ray crystal structure of TATB includes two molecules per unit cell (triclinic) with parameters $a = 9.010$ Å, $b = 9.028$ Å, $c = 6.812$ Å, and $\alpha = 108.59°$, $\beta = 91.82°$, and $\gamma = 119.97°$.[11]

We conducted several simulations with specified shock speeds of 8, 9, and 10 km/s on a (1,1,2) supercell in the (*a*,*b*,*c*) lattice directions, respectively. These shock speeds are near and above the detonation velocity of TATB, measured at 7.76 km/s.[24] This simulation cell contained four TATB molecules whose initial positions were taken from the experimentally determined X-ray crystal structure.[11] The crystal structure of TATB has been determined to include two molecules per unit cell, a triclinic structure with lattice parameters $a = 9.010$ Å, $b = 9.028$ Å, $c = 6.812$ Å, and $\alpha = 108.59°$, $\beta = 91.82°$, and $\gamma = 119.97°$.[11] In vector form, the lattice vectors of the computational unit cell are $a = (7.59911, -4.8449, 0.2862)$ Å, $b = (0, 8.557, -2.8781)$ Å, $c = (0, 0, 13.624)$ Å. This work primarily focuses on planar shock propagation down the *c*, or *z*, direction. We have also performed a simulation for a shock propagating in the y direction, most closely aligned with the *b* lattice vector. We also simulated a larger supercell of dimension (1,2,2), containing eight TATB molecules (as in Figure 1b), with a shock speed of 10 km/s. We used the quantum-based, self-consistent charge density-functional tight binding (SCC-DFTB) method to calculate the interatomic forces.[12] This method allows for the description of total energies, atomic forces, and charge transfer in a self-consistent manner. It has been successfully tested on organic and bioorganic systems[13,14] and has been shown to accurately predict reaction energies.[12] Application of this method to the study of nitromethane, an explosive material of similar elemental composition as TATB, under pressure has yielded comparable results to those obtained from density functional calculations.[15,16]

We performed MD simulations with a time step of 0.5 fs for up to 430 ps with shock speeds of 8 and 9 km/s, and 202 ps for a shock speed of 10 km/s on the $1 \times 1 \times 2$ smaller computational cell. For the larger $1 \times 2 \times 2$ supercell, the simulation was conducted up to 140 ps. In all simulations, initial position of TATB molecules were taken from the experimental X-ray structure and then optimized with the SCC-DFTB method. Initial velocities were randomly chosen, with an initial temperature of 300 K. We then performed an equilibration for a period of up to 2 ps at temperature of 300 K. Shock compression occurred along the *c* (*z*) lattice direction in all simulations except one. For comparative purposes, we also conducted a simulation on a $1 \times 2 \times 2$ supercell in the *y* lattice direction (most closely aligned with *b* axis) for a period of 80 ps. We implemented a procedure to identify stable molecular species based on bond-length and lifetime criteria: two atoms were counted as bonded if their distance was less than a critical value r_c. For atoms bonded to hydrogen the distance criterion must be met for at least 20 fs, while bonds not involving H (e.g., C−C, N−O, etc.) must survive 45 fs. These time scales were chosen to be characteristic of a few molecular vibrations. r_c was determined to be the first maximum in the calculated element-element potential of mean force. Further, molecules were required to meet a minimum lifetime of 100 fs before being identified.

Fast energy transfer processes,[17] such as phonon generation, up-pumping, and intramolecular vibrational energy redistribution are most likely manifested in the early stages of the reaction zone.[18] During this stage, the explosive initial response to a weak shock may be affected due to microscopic properties such as the crystal structure, electrostatic potential,[19] charge distributions,[20] and π-stacked interactions,[21] among others. The later stage, however, is dominated by complex chemical reactions that lead to products such as H_2O, N_2, CO_2, and large clusters. Relatively few studies have been performed on the chemistry of stronger shocks due to the more challenging time scales involved and requirement for accurate methods of simulating a variety of chemical reactions,[22,23] and our reported simulations are the first to probe the formation of stable products in an insensitive high explosive under conditions of a steady shock.

Figure 2 displays the time evolution of the average temperature, stress, and volume for all three initial shock speeds. For

(12) Elstner, M.; Porezag, D.; Jungnickel, G.; Elsner, J.; Hauk, M.; Frauenheim, T.; Suhai, S.; Seifert, G. *Phys. Rev. B* **1998**, *58*, 7260.
(13) Elstner, M.; Hobza, P.; Frauenheim, T.; Suhai, S.; Kaxiras, E. *J. Chem. Phys.* **2001**, *114*, 5149.
(14) Cui, Q.; Elstner, M.; Kaxiras, E.; Frauenheim, T.; Karplus, M. *J. Phys. Chem. B* **2001**, *105*, 569.
(15) Margetis, D.; Kaxiras, E.; Elstner, M.; Frauenheim, T.; Manaa, M. R. *J. Chem. Phys.* **2002**, *117*, 788.
(16) Reed, E. J.; Joannopoulos, J. D.; Fried, L. E. *Phys. Rev. B* **2000**, *62*, 16500.
(17) Tarver, C. M. *J. Phys. Chem.* **1997**, *101*, 4845.
(18) Dlott, D. D.; Fayer, M. D. *J. Chem. Phys.* **1990**, *2*, 3798.
(19) Politzer, P.; Murray, J. S. In *Theoretical and Computational Chemistry: Energetic Materials*, Part 2; Politzer, P., Murray, J. S., Eds.; Elsevier: Amsterdam, 2003.
(20) Rice, B. M.; Hare, J. J. *J. Phys. Chem. A* **2002**, *106*, 1770.
(21) Zhang, C.; Wang, X.; Huang, H. *J. Am. Chem. Soc.* **2008**, *130*, 8359.
(22) Strachan, A.; van Duin, A.; Chakraborty, D.; Dasgupta, S.; Goddard, W. A., III *Phys. Rev. Lett.* **2003**, *91*, 098301.
(23) Nomura, K.; Kalia, R. K.; Nakano, A.; Vashishta, P.; van Duin, A.; Goddard, W. A. *Phys. Rev. Lett.* **2007**, *99*, 148303.

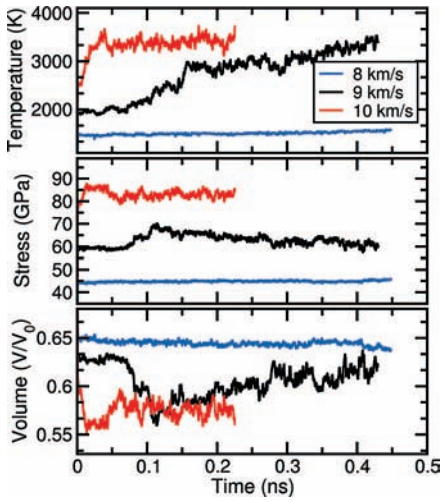

Figure 2. Time evolution of average temperature, shock-propagation-direction stress, and volume of $1 \times 1 \times 2$ computational cell for simulations at shock speeds of 8, 9, and 10 km/s. The initial cell volume (V_0) is 884.97 Å^3.

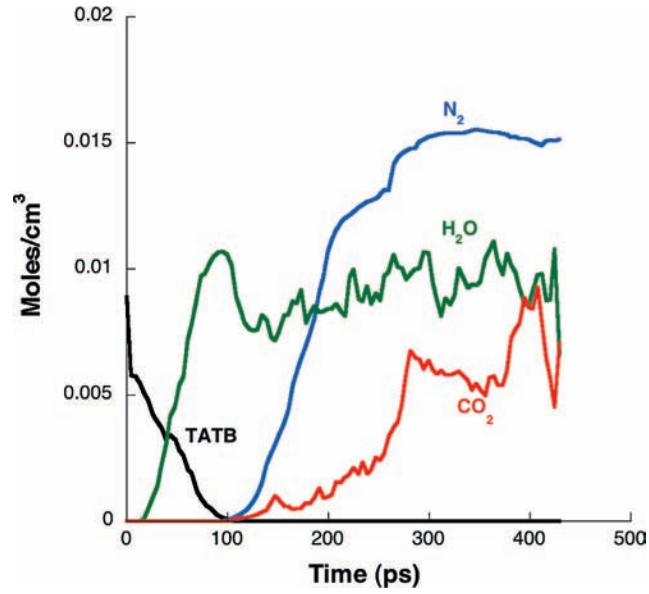

Figure 3. Calculated concentration time profile of reactants (TATB) and most dominant gas products N_2, H_2O, and CO_2, at shock speed of 9 km/s.

the 9 km/s shock speed simulation, the temperature gradually increases from around 1900 to 3500 K, while the stress increases from 58 to 70 GPa, as a result of chemical reactions. More dramatic conditions are noted for the 10 km/s shock speed simulation, where the temperature increases from around 2500 to 3500 K at half the simulation duration of the 9 km/s shock speed, and the stress reaches 85 GPa in less than 50 ps of simulation time. These overdriven conditions of temperature and pressure are far above steady detonation for TATB, which occurs at a shock speed of about 7.7 km/s (at $\rho = 1.88$ g/cm^3) and a pressure of 29 GPa.[24] Our results indicate sub-nanosecond reactivity for overdriven single-crystal TATB. For the 8 km/s simulation, the temperature and stress maintain near-constant values of 1500 K and 42 GPa throughout the simulation period. We note that the only observed reactivity at this shock speed is protons transfer between amino and nitro groups up to 0.43 ns of simulation time. Clearly, chemical transformations occur faster as the shock speed increases, due to the more rapid rise in temperature and stress.

The lack of irreversible decomposition at shock speeds closer to detonation may be due to the lack of defects, such as voids, in the crystal.[25] Defects, voids, and other sources of hot spots are well known to play key roles in sustaining chemical reactions in shocks at experimentally observed detonation speeds, while perfect crystals (such as those we simulate) require much higher shock speed for detonation reaction. Voids and defects sizes are in the micrometer scale, and their inclusion in similar concentrations as usually encountered in shock experiments is computationally prohibitive at the level of treatment that we use. Nevertheless, our results do indicate that a transition from void-induced (hot spot) chemistry to initiation of the bulk crystal could occur between 8 and 9 km/s.

As noted above, the multiscale method allows simulations of several hundred picosecond duration.[9] Figure 3 displays the reaction of TATB to form small stable product molecules for a shock with a speed of 9 km/s, the longest simulation having a significant population of products. As shown, water is the first stable product to form after 30 ps, accompanied by the formation of mono- and dibenzofurazans (not shown). Experimental evidence for benzofurazans have been reported for decomposing TATB subjected to various stimuli such as heat, impact, or UV photolysis.[26] Density functional calculations also showed that intramolecular hydrogen transfer is a rate-limiting step with a barrier of 47.5 kcal/mol, and a precursor to further decomposition of TATB toward H_2O and benzofurazans.[27] We note that oscillation in the water concentration throughout the simulation is mainly due to dissociation−recombination reactions of the type $H_2O \leftrightarrow H + OH$. Most of H_2O is formed before the appearance of N_2, and later CO_2, at about 120 ps of simulation time. Once hydrogen is eliminated from amine groups to form water, nitrogen of adjacent molecules joins in to form N_2. Both H_2O and N_2 appear to reach a steady state of concentration at 100 and 250 ps, respectively. Unlike water, however, the formation of N_2 does not proceed before a polymerization process is underway in which the heavy fragments of the parent TATB have all bonded together.

The most striking feature in this simulation is the formation of nitrogen-rich heterocyclic clusters of various sizes. Figure 4 shows the time evolution of the size of carbon-containing clusters, indicated with the actual number of carbon atoms in a cluster. The plot color indicates the ratio of average nitrogen to carbon content in these clusters, averaged over a period of 1 ps. We define a cluster as any species with at least 6 carbon atoms. Prior to 80 ps of simulation time, TATB molecules are shown in a red color that corresponds to 1:1 ratio of nitrogen/carbon. Carbon clustering begins when fragments of two TATB molecules are bonded (12 C atoms) and then three (18 C atoms) and so on. At about 100 ps, large carbon clusters dominate, some including all the available carbon in the cell, followed by a slow *decrease* in cluster size with time due to formation of CO_2. This is in contrast with prior models of carbon cluster formation, which include only diffusion-limited cluster growth.[2]

(24) Dobratz, B. M.; Crawford, P. C. *LLNL Explosive Handbook*; UCRL-52997, University of California: Livermore, CA, 1985.
(25) Bowden, F. P.; Yoffe, A. D. *Initiation and Growth of explosion in liquids and solids*; Cambridge University Press: Cambridge, 1952.
(26) Sharma, J.; Forbes, J. W.; Coffey, C. S.; Liddiard, T. P. *J. Phys. Chem.* **1987**, *91*, 5139.
(27) Wu, C. J.; Fried, L. E. *J. Phys. Chem. A* **2000**, *104*, 6447.

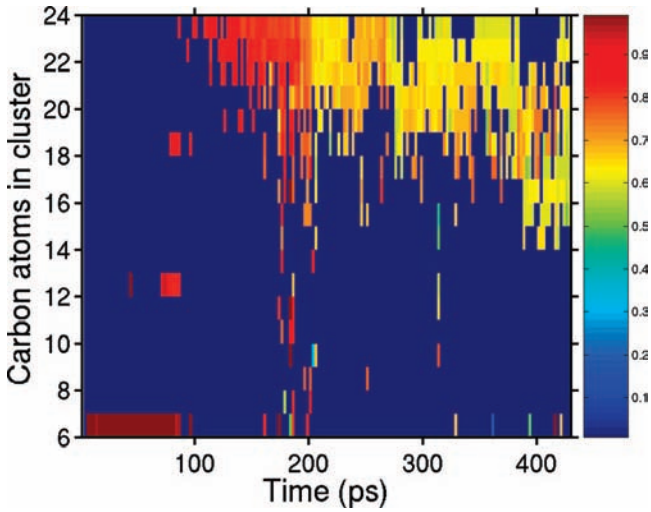

Figure 4. Time evolution of the size of carbon-containing clusters in the 1 × 1 × 2 computational cell (with initial total of 24 carbon atoms) for the 9 km/s simulated shock. The plot color indicates the ratio of average nitrogen to carbon contents in these clusters, averaged over a period of 1 ps. Individual TATB molecules, each containing six carbon and six nitrogen atoms, are shown in a red color that corresponds to 1:1 ratio of nitrogen to carbon prior to 80 ps of simulation time.

The transition from red to yellow in the figure also indicates decreasing average nitrogen content in these clusters due to the production of N_2.

Some heterocycles persist throughout the simulation. To illustrate, the cluster with 22 carbon atoms first appears after 90 ps from the start of the simulation with a stoichiometric composition $C_{0.92}H_{0.54}N_{0.83}O_{0.71}$, and last appears with the composition $C_{0.92}H_{0.08}N_{0.58}O_{0.42}$ after 423 ps of simulation time. Changes in composition occur throughout the simulation, and are expected due to reactivity of species that have not reached chemical equilibrium, and also due to steady temperature increases. In this simulation, however, we find that a persistent cluster with the highest concentration occurs during the last 40 ps of the simulation period, and has the composition of $C_{15}N_9O$. Further, these size-varying clusters are very stable, as indicated by their persistence at temperatures as high as 3500 K. Near the end of this simulation, most hydrogen atoms have been consumed in the formation of water (some in the form of H_3O and OH), and 58% of nitrogen forming N_2, along with single intermediates such as NCO, NCO_2, and CN_2. The carbon contents in these, along with that in CO_2 represent only 29% of the total carbon available. The remaining 71% of carbon, 42% of nitrogen, along with less than 10% of oxygen are sequestered in the nitrogen heterocycles.

In Figure 5, we compare the results obtained from simulations of cell sizes of 1 × 1 × 2 (4 TATB molecules) and 1 × 2 × 2 (8 TATB molecules) for a shock speed of 10 km/s. Since the two simulations differ in the total number of atoms, and in order to facilitate direct comparison, we plot the time evolution of the fractional carbon content in carbon-containing clusters with respect to total available the computational cell (Figure 5a), and the time profile of the average nitrogen to carbon ratio in these clusters (Figure 5b). As shown, both simulations confirm the formation of nitrogen-rich heterocycles, albeit at different time due to increased reactivity with increase in the shock speed. Figure 5a, for example, shows almost identical fractional distribution to total carbon between 10 and 40 ps of simulation time of 0.8−1 in the two simulations. This corresponds to

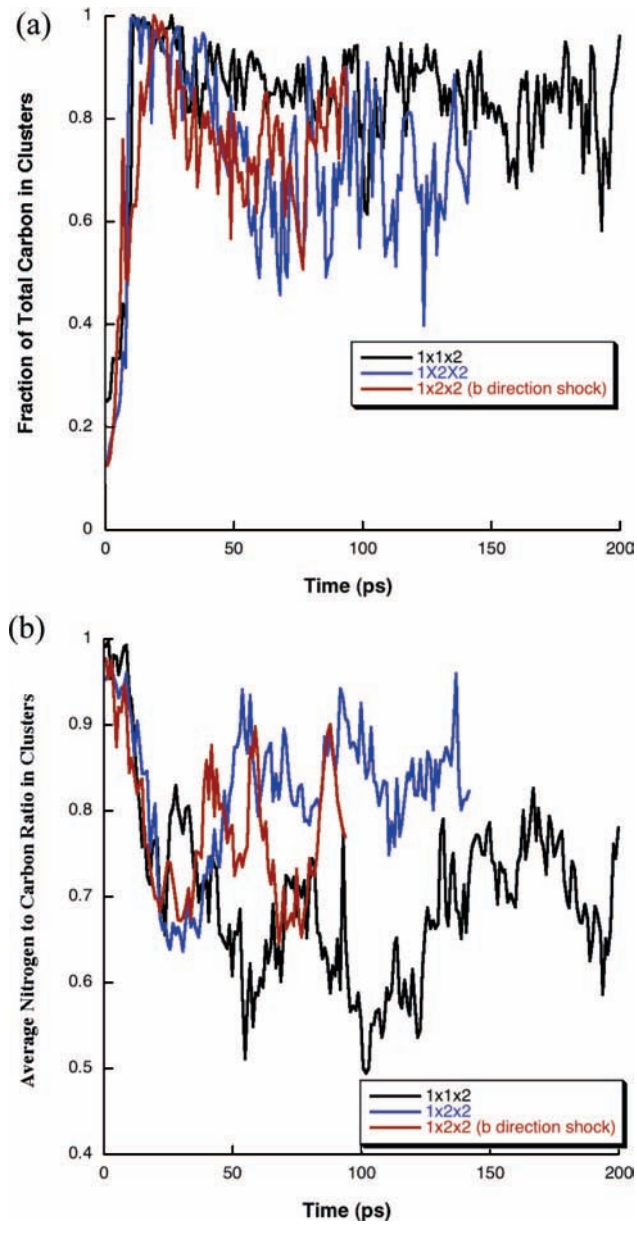

Figure 5. Time evolution of (a) carbon fractional distribution in carbon-containing clusters with respect to total available in the computational cell (24 C atoms in 1 × 1 × 2, and 48 C atoms in the 1 × 2 × 2 cell), and (b) the average nitrogen/carbon ratio in these clusters obtained from simulated shocked TATB experiencing a shock wave speed of 10 km/s in the *z* and *y* directions (most closely aligned with the *c* and *b* lattice vectors, respectively).

clusters of varying carbon content between 19C to 24C in the 1 × 1 × 2 cell, and 38C to 48C in the larger 1 × 2 × 2 supercell. For the total duration of the two simulations, the carbon content in these clusters varies dynamically between 14C and 24C for the 202 ps simulation of the smaller 1 × 1 × 2 cell, and between 19C and 48C for the 140 ps simulation of the larger 1 × 2 × 2 cell. Similarly, Figure 5b shows the nitrogen contents variation in these clusters, ranging between 12N (50% N) and 24N (100% N) in the smaller cell simulation, and between 30N (63% N) and 46N (96% N) in the larger 1 × 2 × 2 simulation cell. In both figures, shock compression along the *y* vs the *z* lattice directions does not seem to provide any significant deviation for the observation of high-nitrogen cluster formation at these shock conditions.

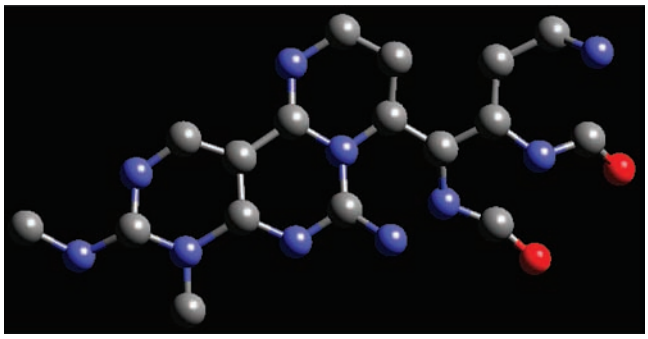

Figure 6. Representative nitrogen-rich heterocycle near the end of simulated TATB experiencing a steady shock wave with a speed of 9 km/s.

The persistence formation of nitrogen-rich large clusters so late during the simulations, with temperature as high as 3500 K is a testament to their resiliency toward further decomposition and further retardation of chemical reactivity of TATB. An example heterocycle structure is presented in Figure 6 obtained from simulated TATB experiencing a steady shock wave with a speed of 9 km/s. It is possible that the heterocycles could be a precursor to a highly stable carbon nitride phase in shocked TATB.[28] The alternation of C−N bonds in the cluster implies that further decomposition to N_2 and pure graphitic carbon clusters, a percolation of sort, require many further mechanistic steps at time-scales well beyond those studied here.

The results of our simulations clearly reveal high concentrations of nitrogen-rich heterocyclic clusters in the simulated shock speeds of 9 and 10 km/s, and that the formation of such clusters is not affected by the atomic size of the simulation cell. Increasing the shock speed has the effect of raising the temperature and the stress experienced by the TATB molecules more rapidly. Although complex chemical transformations are occurring continuously in the dynamical, high temperature, reactive environment, a simple overall scheme for the decomposition of TATB under shock conditions emerges from these simulations. First, water is the earliest decomposition products, resulting from both inter- and intrahydrogen transfers that also deplete the reacting TATB from its peripheral hydrogen and oxygen constituents in the amino and nitro groups. Second, once most of the water has been formed, a polymerization process is initiated in which several TATB remaining fragments are joined together. This is the beginning step in the formation of high-nitrogen clusters. Depending on the configurational interactions in this step (e.g., N−N, C−N, or C−O), further products such as N_2 and CO_2 are formed. Third, the remaining clusters with high concentration of carbon and nitrogen (and little oxygen) remain dynamically stable. It is this step, hitherto unknown, that our simulations have revealed. As noted above, further decomposition of these clusters to form final products of N_2, CO (or CO_2), and particulate carbon will eventually occur, but require many mechanistic steps. The representative nitrogen-rich cluster in Figure 6 is but an illustrative example on the mechanistic complexity that might be envisioned in the formation of gaseous N_2 product.

Chemical equilibrium calculations suggest that TATB would decompose into $3H_2O + 3N_2 + CO + CO_2 + 4C$.[29] We have shown here that most of the carbon and nitrogen are instead locked in nitrogen-rich heterocycles on the time scale of up to 400 ps in the case of simulated TATB experiencing a steady shock with a speed of 9 km/s. In addition, we find that cluster size decreases as chemical composition shifts toward pure carbon for this particular shock speed. Assuming that all nitrogen encountered in the heterocycles will ultimately react to form N_2, it is notable that the final products of our simulation would follow a similar decomposition trend. Two-thirds of the initially available carbon will ultimately be liberated in some of its known phases such as graphitic clusters, as was recently reported in thermal decomposition simulations.[30] We are currently extending our simulations to follow further decomposition of the nitrogen-rich heterocycles in order to scrutinize the characteristics of carbon clusters as they evolve during the explosive reactivity of TATB.

Acknowledgment. This work performed under the auspices of the U.S. Department of Energy Lawrence Livermore National Laboratory under Contract No. DE-AC52-07NA27344.

JA808196E

(28) Niu, C.; Lu, Y. Z.; Lieber, C. M. *Science* **1993**, *261*, 334.

(29) Cooper, P. W.; Kurowski, S. R. *Introduction to the Technology of Explosives*; Wiley-VCH, Inc.: New York, 1996.

(30) Quenneville, J.; Germann, T. C.; Thompson, A. P.; Kober, E. M. In *Shock Waves in Condens. Matter*; AIP: New York, 2007; p 451.